

# The mechanism of turbulent drag reduction with wall oscillation

Kwing-So Choi \*, Brian R. Clayton

*School of Mechanical, Materials, Manufacturing Engineering and Management, University of Nottingham, University Park, Nottingham NG7 2RD, UK*

Received 16 February 1999; accepted 23 July 2000

## Abstract

An extensive study of the near-wall structure of turbulent boundary layer over a spanwise oscillating wall was conducted using hot-wire measurements in a wind tunnel in order to better understand the mechanisms involved in turbulent drag reduction under these conditions. The results showed that the logarithmic velocity profiles were shifted upwards and the turbulence intensities reduced, suggesting that the viscous sublayer was thickened as a result of drag reduction with wall oscillation. The probability density functions of velocity fluctuations exhibited long tails of positive probability, reflecting increases in the skewness and kurtosis within the viscous sublayer. The measured thickness of the Stokes layer was comparable to that of the viscous sublayer of the boundary layer when the turbulent drag reduction was observed with the wall oscillation. At the same time, the Reynolds number of the Stokes layer was found well below the critical value, so that the Stokes layer was expected to remain laminar if there were no boundary layers over the oscillating surface. These are considered to be important conditions in obtaining turbulent drag reduction with spanwise-wall oscillation. The present study also showed that a net spanwise vorticity was generated by the periodic Stokes layer over the oscillating wall just outside the viscous sublayer, which reduces the mean velocity gradient of the boundary layer near the wall. At the same time, the spanwise vorticity hampers the longitudinal vortices in the viscous sublayer to stretch in the streamwise direction, reducing the streamwise vorticity associated with these vortices. The *near-wall burst* activity was weakened as a result of this, resulting in the reduction of turbulent skin-friction drag. A remarkable change in the burst signature in the near-wall region of the boundary layer was observed. © 2001 Elsevier Science Inc. All rights reserved.

**Keywords:** Turbulence; Turbulence structure; Boundary layer; Drag reduction; Wall oscillation

## 1. Introduction

Akhavan and her colleagues (Jung et al., 1992) at the University of Michigan recently conducted a direct numerical simulation (DNS) study, demonstrating that the skin-friction drag of a turbulent channel flow can be reduced by oscillating one of the walls in the spanwise direction. Their results show that a 40% reduction in turbulent skin-friction drag can be obtained only after five periods of spanwise-wall oscillation with the non-dimensional period  $T^+$  set at 100. The logarithmic velocity profile of the channel flow is shifted upwards, suggesting that the viscous sublayer is thickened as a result of the spanwise-wall oscillation. It is also shown that the intensities of velocity fluctuations are reduced by up to 30%. The basic findings of this investigation were later confirmed by Baron and Quadrio (1996) in their DNS study. They also investigated the effect of the wall velocity on the total energy balance of this drag-reduction technique and found that net energy savings are possible at a low wall-oscillation velocity.

Indeed, there was a 10% net energy saving by the spanwise-wall oscillation at the wall velocity of  $Q_w/8h$ . No net savings were obtained, however, when the wall velocity was greater than  $3Q_w/8h$ .

These numerical simulations were followed by an experimental investigation by Laadhari et al. (1994), which demonstrated that the mean velocity gradient of the boundary layer is reduced near an oscillating wall. The reductions in turbulence intensities across the boundary layer were also shown, suggesting that the skin-friction drag of the turbulent boundary layer may be reduced by the spanwise-wall oscillation. The reduction of skin-friction drag in the turbulent boundary layer with spanwise-wall oscillation was later confirmed by Choi et al. (1998) in their experimental study. They measured the streamwise variation of wall-shear stress over an oscillating plate and showed that the skin-friction coefficient begins to reduce just upstream of the leading edge to reach the maximum level of drag reduction near the middle of the plate. Their results indicate that the skin-friction coefficient is reduced by as much as 45% compared with a stationary wall. This agrees closely with those obtained from direct numerical simulations (Jung et al., 1992; Baron and Quadrio, 1996). The skin-friction coefficient seems to revert back gradually towards the original level with almost a 20% reduction in skin-friction coefficient

\* Corresponding author. Tel.: +44-115-951-3792; fax: +44-115-951-3800.

E-mail address: kwing-so.choi@nottingham.ac.uk (K.-S. Choi).

**Notation**

$f$	frequency of spanwise-wall oscillation
$h$	channel half height
$H$	boundary-layer shape factor
$k$	threshold value in the VITA technique
$Q_x$	channel flow rate per unit width
$R_\theta$	Reynolds number based on the momentum thickness
$T$	time
$T^+$	non-dimensional time, $Tu^{*2}/\nu$
$u$	streamwise velocity
$u^+$	non-dimensional streamwise velocity, $u/u^*$
$u^*$	friction velocity
$u'$	RMS velocity fluctuation
$U_\infty$	freestream velocity

$w$	spanwise velocity
$w^+$	non-dimensional spanwise velocity, $w/u^*$
$x$	streamwise distance, measured from the leading edge of the oscillating plate
$y$	normal distance
$z$	spanwise distance
$x^+$	non-dimensional distance, $xu^*/\nu$
$y^+$	non-dimensional distance, $yu^*/\nu$
$z^+$	non-dimensional distance, $zu^*/\nu$

**Greeks**

$\Delta z$	amplitude of wall oscillation
$\nu$	kinematic viscosity of the fluid
$\Omega_z$	spanwise vorticity

after more than two boundary layer thicknesses from the trailing edge of the oscillating plate.

It must be mentioned here that the original DNS study by Jung et al. (1992) was conducted over a stationary channel wall with oscillating cross-flow, except for a special case where one of the channel walls was oscillated in the spanwise direction. On the other hand, all the numerical simulations by Baron and Quadrio (1996) were carried out in a turbulent channel flow with spanwise-wall oscillation. The previous experimental studies (Laadhari et al., 1994; Choi et al., 1998) as well as the present work reported here were conducted in a wind tunnel by oscillating a boundary-layer wall in the spanwise direction.

The average spanwise spacing between low-speed streaks of the turbulent boundary layer is approximately 100 wall units (Kline et al., 1967). These streaks are formed close to the wall on the upwash side of longitudinal vortices, either singularly or as a pair (Blackwelder and Eckelmann, 1979; Smith and Schwartz, 1983; Kim, 1983). Using the conditional correlation of wall-shear stress in the turbulent boundary layer, it was indeed demonstrated that the spanwise correlation distance of longitudinal vortices is approximately 50 wall units (Choi, 1989), one half of the average spacing between the low-speed streaks. A similar result has recently been reported by Jeon et al. (1999) in their analysis of DNS database for turbulent channel flow. It was considered, therefore, that the sequence of the near-wall turbulence events may be disturbed if the wall surface moves suddenly by more than 50 wall units in the spanwise direction (Choi, 1996). In other words, the spatial coherence between the longitudinal vortices and low-speed streaks can be disrupted by oscillating a wall in the spanwise direction (Baron and Quadrio, 1996). In practice, the speed of the wall oscillation depends on the type of oscillating mechanism being used. Therefore, both the wall-oscillation frequency and amplitude are important parameters in obtaining drag reductions using spanwise-wall oscillation (Choi et al., 1998).

It is known that the Reynolds stress of the three-dimensional turbulent boundary layer over a swept wing of an aircraft is less than that of the two-dimensional boundary layer. It is suggested (Schwarz and Bradshaw, 1994) that this is caused by a modification of the quasi-streamwise vortices in the near-wall region by the spanwise shear of the three-dimensional boundary layer. Based on the experimental data, Eaton (1995) conjectured that the cross-flow of the three-dimensional boundary layer inhibits the generation of low-speed streaks and eliminates the ejections. The DNS results (Sendstad, 1992) seem to show that the streamwise vortices are shifted laterally with respect to the wall layer streaks below them. This causes the vortices to pump high- rather than low-speed fluid away

from the wall, and to splash low- rather than high-momentum fluid towards the wall, thereby reducing the production of the Reynolds stress in the near-wall region of turbulent boundary layer. However, the modification of near-wall turbulence structure by the spanwise shear of a steady, three-dimensional boundary layer is rather subtle, possibly because the realignment angle of the longitudinal vortices by the spanwise shear over a swept wing is not very large.

The objective of the present investigation is to better understand the mechanism of turbulent drag reduction of the boundary layer by spanwise-wall oscillation. In order to achieve this objective, an extensive study of the near-wall structure of the boundary layer modified by the wall oscillation was carried out with hot-wire anemometry using single and cross-wire sensors. Profiles of mean velocity and turbulence intensity and the higher-order statistics of velocity fluctuations were obtained when the wall was oscillated in the spanwise direction at different frequencies. The energy spectra and probability density functions of velocity fluctuations were also documented over an oscillating wall and they were compared with those without wall oscillation. The phase-averaged velocity profiles were then obtained over a period of wall oscillation and the conditionally averaged burst signatures were studied in order to investigate the effect of spanwise-wall oscillation on the near-wall turbulence activities. Finally, a possible drag reduction mechanism by spanwise-wall oscillation is proposed based on the present and previous experimental findings.

## 2. Experiments

The experiments were performed in an open-return, low-speed wind tunnel at the University of Nottingham with a 300 mm × 534 mm working-section, 3.0 m long. The boundary layer was tripped at the inlet of the working-section to ensure a fully developed turbulent boundary layer over the test surface. The leading edge of the 500 mm long oscillating plate was located 2 m downstream of the trip, set flush to the surrounding surface. The freestream velocity of the present investigation was nominally 2.5 m/s with a corresponding Reynolds number  $R_\theta = 1190$  based on the momentum thickness. The pressure gradient along the length of the working-section was nearly zero, with the shape factor of the boundary layer  $H = 1.44$  at the trailing edge of the oscillating plate. The sinusoidal oscillation was produced by a crank-shaft system, with oscillation frequencies up to 7 Hz and peak-to-peak amplitudes up to 70 mm.

The streamwise velocity measurements were made with the Dantec 56C CTA system using a single, miniature, hot-wire probe (Dantec 55P15). This sensor had a  $5\text{ }\mu\text{m}$  diameter sensing element,  $1.2\text{ mm}$  long, which was operated in constant temperature mode with an over-heat ratio of 1.8. Measurements of spanwise velocities were made with a subminiature X-wire probe, purpose-made by Dantec, which had a  $2.5\text{ }\mu\text{m}$  diameter sensing element,  $0.5\text{ mm}$  long. The total length of the gold-plated wires was  $1.5\text{ mm}$  with a space of  $0.5\text{ mm}$  between the two wires. The X-wire probe was operated at an overheat ratio of 1.5 to reduce the thermal cross-talk, but was sufficiently sensitive to velocity fluctuations. The data from the anemometer were sampled at a rate of  $2\text{ kHz}$  through IOTech ADC 488/8S analogue-to-digital converter.

Wall-shear stress was determined by the near-wall slope of the boundary-layer profile obtained from a single hot-wire measurement. The Preston tubes of  $1.24$  and  $2.01\text{ mm}$  outer diameter were also used for the wall-shear stress measurement in the turbulent boundary layer with and without wall oscillation. The total pressure from the Preston tube and the static pressure from the Pitot static tube placed right above it in the boundary layer were connected to a differential pressure transducer (Furness Control FC0510), which is accurate to  $0.25\%$  of the pressure reading with  $0.001\text{ Pa}$  resolution. The agreement of the wall-shear stresses between these two techniques was typically within  $5\%$  of the reading.

### 3. Results and discussion

The mean-velocity profiles of the boundary layers with spanwise-wall oscillation are shown in Fig. 1 in a log-law plot, where all the profiles were non-dimensionalised using the friction velocity for each oscillating condition. The friction velocities used in this figure were determined from the near-wall slope of the boundary-layer profile, except for the case without wall oscillation, where the Clauser-plot method was used. The curves drawn through the data (Dean, 1976) cover the entire region of the boundary layer including the viscous sublayer, which seem to fit all the profiles very well. The logarithmic velocity profiles are shifted upwards with an increase in oscillation frequency, suggesting that the viscous sublayer is thickened by the spanwise-wall oscillation. When the outer-scaled velocity profiles are plotted in linear coordinates, the mean velocity gradient in the near-wall region was found to be

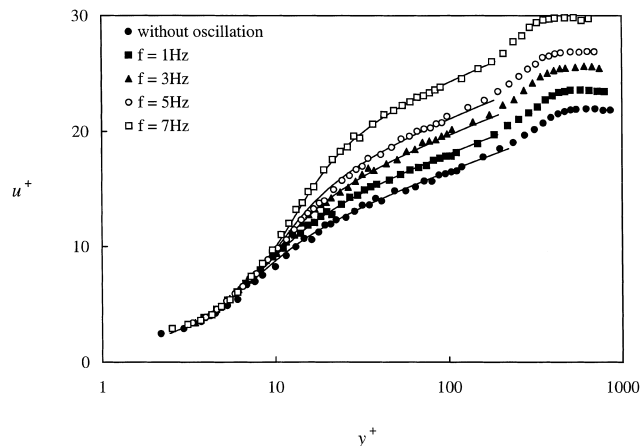


Fig. 1. Logarithmic velocity profiles of the boundary layer  $10\text{ mm}$  downstream from the trailing edge of the oscillating plate, for different frequencies of wall oscillation ( $\Delta z = 70\text{ mm}$ ).

significantly reduced with wall oscillation (Choi et al., 1998). This reduction in the mean-velocity gradient, which is also seen in the experimental results of Laadhari et al. (1994), clearly demonstrates that the wall-shear stress of the turbulent boundary layer is reduced by the spanwise-wall oscillation. The inner-scaled velocity profiles showed, on the other hand, that the extent of linear region of the viscous sublayer is increased from  $y^+ \approx 2.5$  without wall oscillation (Durst et al., 1995) to  $y^+ \approx 10$  for the maximum oscillation frequency (Choi et al., 1998).

The turbulence intensities of the boundary layer are plotted in Fig. 2 against the non-dimensional distance  $y^+$  from the wall, where large reductions in the intensity values are evident within the inner region when the wall is oscillated in the spanwise direction. The experimental results by Laadhari et al. (1994) as well as numerical data by Jung et al. (1992) and Baron and Quadrio (1996) exhibit similar behaviour showing the reductions in turbulence intensities in all three components. The reductions in turbulence intensities by spanwise-wall oscillation are clearly demonstrated in the energy spectra of velocity fluctuations at  $y^+ = 1.5$ ,  $4$  and  $20$  (Figs. 3(a)–(c), respectively). Here, the energy spectra shown here are defined in such a way that their integral over the entire frequency will give the mean square value of  $u$ -component velocity. It seems that the turbulence energy is dramatically reduced at low frequencies, say below  $50\text{ Hz}$  while the energy at higher frequencies is increased. This seems to suggest that there is a transfer of energy from the large-scale to small-scale turbulence eddies by the periodic Stokes layer developed over an oscillating wall. However, this could also be understood that there is less production of large-scale structures due to suppression of an instability mechanism (Schoppa and Hussain, 1998), and increased production of small scales due to augmentation of a different instability mechanism. The spikes in the energy spectrum at  $y^+ = 1.5$  correspond to the frequency of the wall oscillation and its harmonics, which are visible only in the data close to the oscillating wall.

The skewness and kurtosis of the velocity fluctuations in the near-wall region of the boundary layer are increased (Figs. 4 and 5, respectively) with an increase in turbulent drag reduction by spanwise-wall oscillation, agreeing very well with the DNS results of Baron and Quadrio (1996). Similar near-wall behaviour is observed in other drag reducing flows, such as the turbulent boundary layers with long-chain polymers, micro-bubble injection (Pal et al., 1989) and over riblets (Choi, 1989). These results indicate that there is a good correlation between

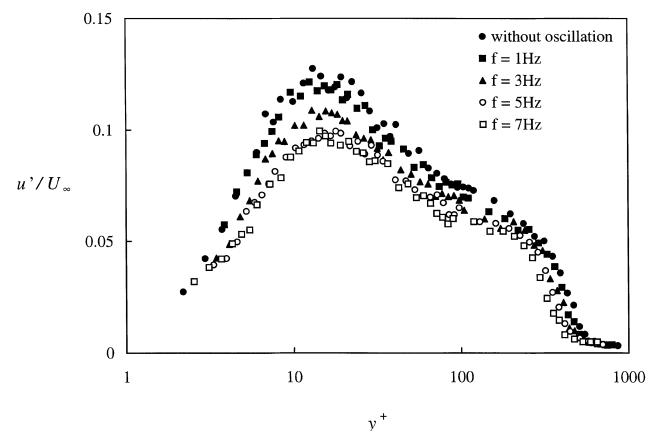


Fig. 2. Turbulent intensity profiles of the boundary layer  $10\text{ mm}$  downstream from the trailing edge of the oscillating plate, for different frequencies of wall oscillation ( $\Delta z = 70\text{ mm}$ ).

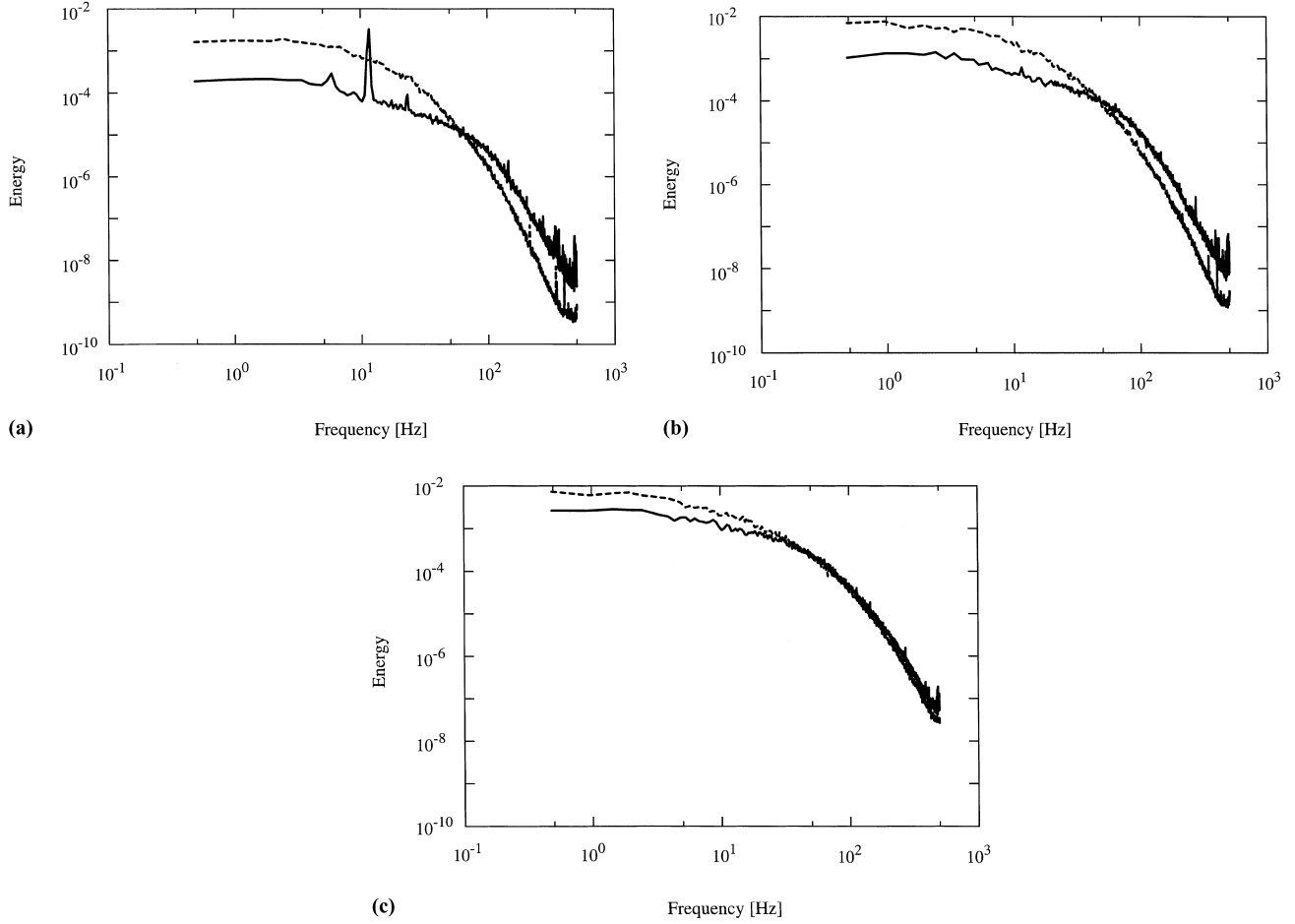


Fig. 3. (a) Energy spectra of  $u$ -component velocity fluctuations at  $y^+ = 1.5$ : – with wall oscillation (over the oscillating plate,  $x = 350$  mm,  $\Delta z = 70$  mm,  $f = 6$  Hz), --- without wall oscillation; (b) energy spectra of  $u$ -component velocity fluctuations at  $y^+ = 4$ : – with wall oscillation (over the oscillating plate,  $x = 350$  mm,  $\Delta z = 70$  mm,  $f = 6$  Hz), --- without wall oscillation; (c) energy spectra of  $u$ -component velocity fluctuations at  $y^+ = 20$ : – with wall oscillation (over the oscillating plate,  $x = 350$  mm,  $\Delta z = 70$  mm,  $f = 6$  Hz), --- without wall oscillation.

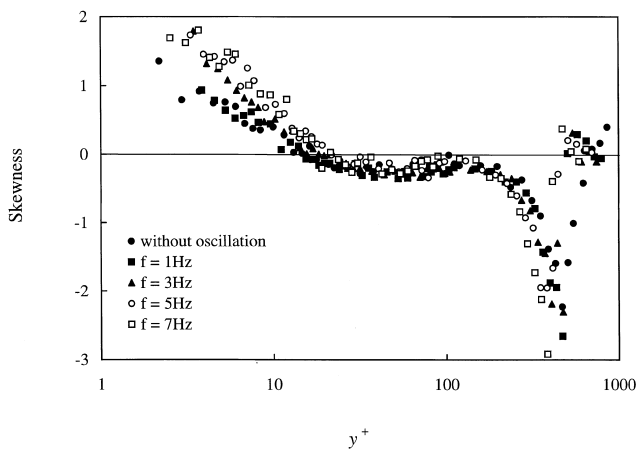


Fig. 4. Skewness profile of  $u$ -component velocity fluctuations in the boundary layer 10 mm downstream from the trailing edge of the oscillating plate for different frequencies of wall oscillation ( $\Delta z = 70$  mm).

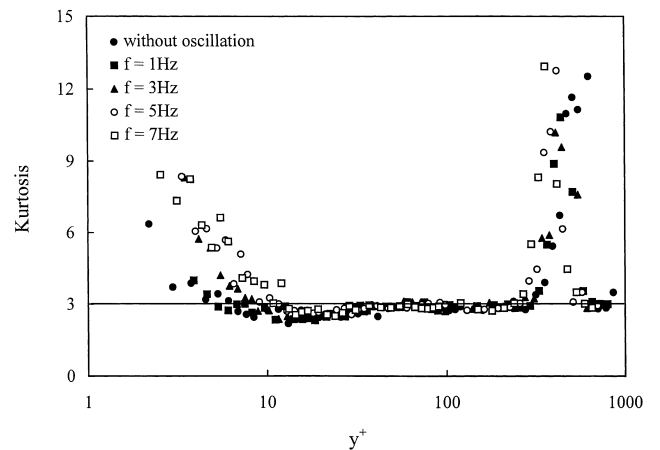


Fig. 5. Kurtosis profile of  $u$ -component velocity fluctuations in the boundary layer 10 mm downstream from the trailing edge of the oscillating plate for different frequencies of wall oscillation ( $\Delta z = 70$  mm).

the increase in the higher moments of turbulence statistics in the near-wall region of the boundary layer and the amount of drag reduction. The probability density function of the velocity fluctuations at  $y^+ = 4$  (Fig. 6(b)) over an oscillating wall ex-

hibits a long tail of positive probability, reflecting an increase in skewness and kurtosis within the viscous sublayer. It indicates that the velocity signal has predominantly positive, spiky excursions in this region of the boundary layer. The proba-

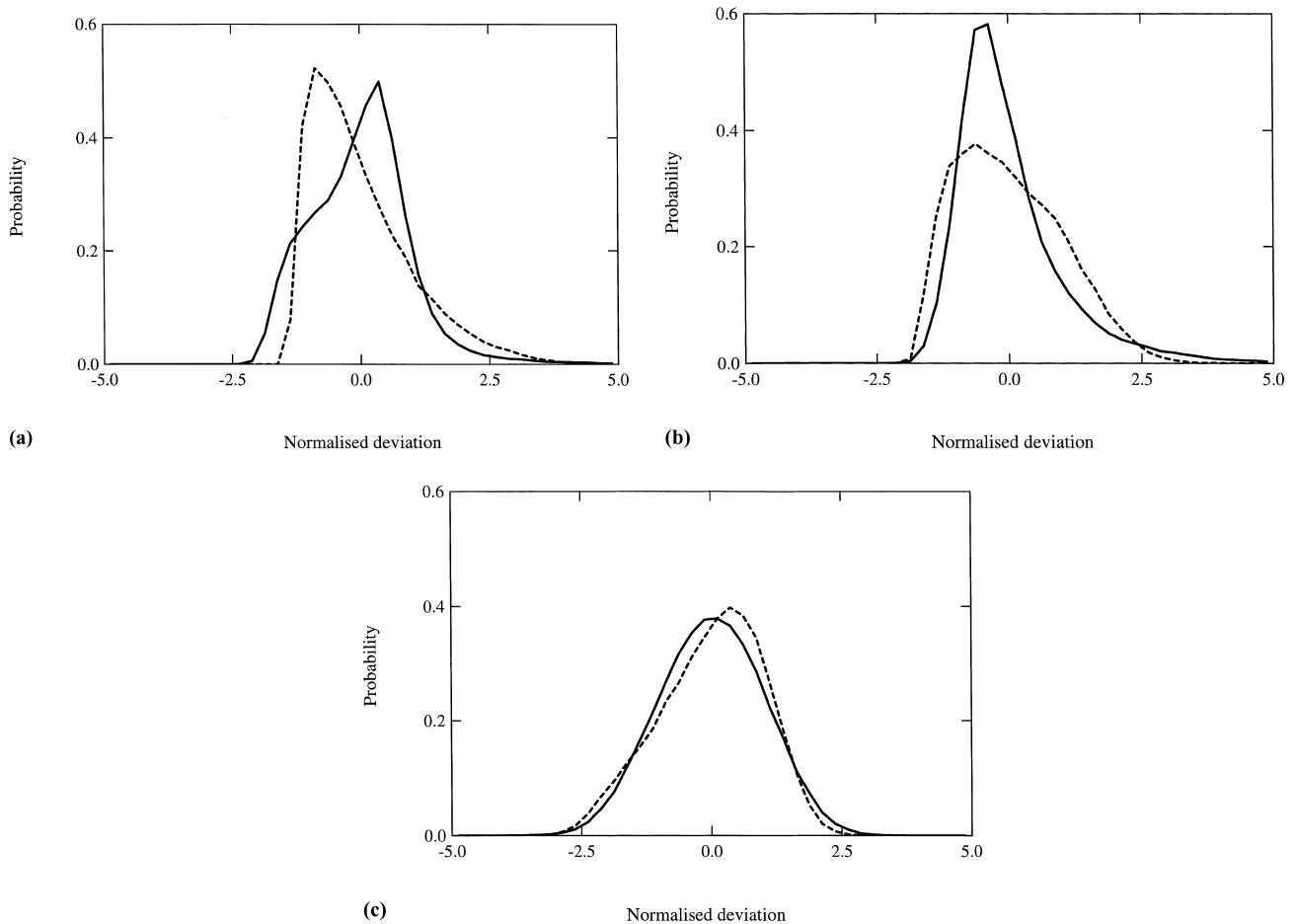


Fig. 6. (a) Probability density functions of  $u$ -component velocity fluctuations at  $y^+ = 1.5$ : – with wall oscillation (over the oscillating plate,  $x = 350$  mm,  $\Delta z = 70$  mm,  $f = 6$  Hz), --- without wall oscillation; (b) probability density functions of  $u$ -component velocity fluctuations at  $y^+ = 4$ : – with wall oscillation (over the oscillating plate,  $x = 350$  mm,  $\Delta z = 70$  mm,  $f = 6$  Hz), --- without wall oscillation; (c) probability density functions of  $u$ -component velocity fluctuations at  $y^+ = 20$ : – with wall oscillation (over the oscillating plate,  $x = 350$  mm,  $\Delta z = 70$  mm,  $f = 6$  Hz), --- without wall oscillation.

bility density function of  $u$ -component velocity fluctuations in the turbulent boundary layer over an oscillating wall is qualitatively similar to that in the three-dimensional turbulent boundary layer. The weighted probability density function in the three-dimensional turbulent boundary layer (Sendstad, 1992) seems to suggest that the turbulence intensity is reduced and the skewness and kurtosis increased within the viscous sublayer as the boundary layer is swept by the spanwise pressure gradient. However, the changes in the turbulence statistics in the three-dimensional boundary layer seem to come mainly from a reduction in the negative-tail probability, while a large increase in skewness and kurtosis in the near-wall region of turbulent boundary layer with wall oscillation is clearly the result of an increase in the positive-tail probability.

The probability density function at  $y^+ = 20$  (Fig. 6(c)) also shows a sign of increase in skewness and kurtosis with a long tail of positive probability, but the difference is not as large at this location of the boundary layer as in the viscous sublayer (Fig. 6(b)). These results are compatible with the measured thickness of the Stokes layer (to be shown later) over the oscillating plate, which only extends to approximately 30 wall units from the wall surface. Here, the Stokes layer thickness is defined as the *depth of penetration* (Schlichting, 1968). This is the distance from the oscillating wall where the local spanwise velocity becomes in phase again with the wall velocity. The

skewness and kurtosis of the velocity fluctuations are even greater closer to the oscillating wall (Figs. 4 and 5), but the elongation of the positive probability tail is not very clear in the probability density function at  $y^+ = 1.5$  (Fig. 6(a)). This is because the velocity signal at this near-wall location is strongly modulated by the oscillation of the Stokes layer. In other words, the probability density function of the velocity fluctuations at  $y^+ = 1.5$  is influenced by a twin-peak probability density function of the sinusoidal wall oscillation (Tennekes and Lumley, 1972), shifting the location of maximum probability to the positive side.

When a flat plate is oscillated tangentially in still fluid, a thin layer of periodic shear flow called the Stokes layer is formed over the plate as a result of viscous diffusion from its surface. In other words, the Stokes layer over an oscillating wall is a constant source of vorticity of alternate signs as the wall moves back and forth (Sherman, 1990) in the spanwise direction. The curves in Fig. 7 show the theoretical, laminar velocity profiles of the Stokes layer over the oscillating wall in still fluid (i.e. without boundary layer flow) at different phases of the wall oscillation. The experimental data for the spanwise velocity profiles are phase averaged over a period of wall oscillation, and are also shown in this figure. It must be pointed out here that the near-wall measurement of  $w$ -component velocity is extremely difficult, which may contain a large amount

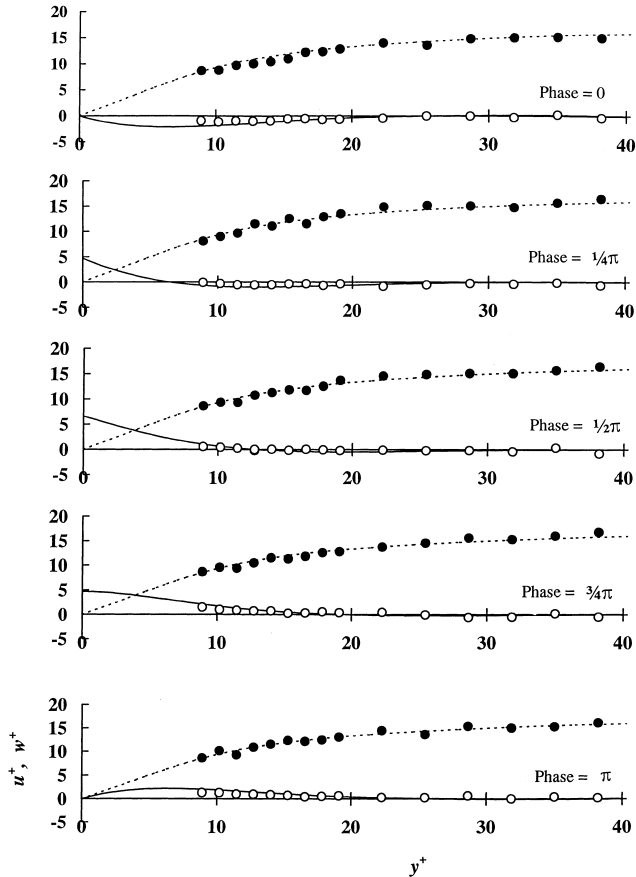


Fig. 7. Velocity profiles in the Stokes layer (over the oscillating plate,  $x = 350$  mm,  $\Delta z = 70$  mm,  $f = 6$  Hz): — Stokes' theory (spanwise velocity profiles),  $\circ$  phase-averaged data ( $w^+$ ), --- Dean's formula (streamwise velocity profiles),  $\bullet$  phase-averaged data ( $u^+$ ).

of error. For the present experiment, however, we have tried to minimise this error by using a subminiature X-wire probe with a 0.5 mm long sensing element with a 0.5 mm spacing between the two wires. The measurement volume of this hot-wire probe is less than four wall units.

It is observed in Fig. 7 that the measured velocity profiles are very similar to the theoretical profiles of laminar Stokes layer. It is also noted that the thickness of the Stokes layer over an oscillating wall is similar to that of the viscous sublayer when turbulent drag reductions are observed. Furthermore, the Reynolds number of the Stokes layer is well below the critical value, so that the Stokes layer is expected to remain laminar (Sarpkaya, 1993; Akhavan et al., 1991a,b) if there were no boundary layers over the oscillating surface. These are considered to be important conditions in obtaining the turbulent drag reduction with spanwise-wall oscillation, since the modification of the near-wall structure seems to result from an interaction of the Stokes layer with the viscous sublayer of the turbulent boundary layer where the majority of the energy production takes place.

The streamwise velocity profiles are also phase averaged over a period of wall oscillation, and are shown in Fig. 7. There appears to be no significant dependence of the velocity profiles on the phase of the wall oscillation outside the viscous sublayer. Examining the phase-averaged velocities closely within the viscous sublayer, however, it is observed that the streamwise velocity profiles exhibit a cyclic change with the change in wall velocity during the oscillation. In other words,

the velocity signal is modulated by the periodic Stokes layer at a frequency twice that of the wall oscillation, which can be seen in the phase-averaged velocity signal over one period of wall oscillation (Fig. 8). The streamwise velocity profile at  $y^+ = 1.5$  seems to be nearly in phase with the spanwise-wall velocity but perhaps with a slight phase lag. At  $y^+ = 4$ , the streamwise velocity is lagged nearly  $\pi/2$  behind the wall velocity. No clear phase relationship between the streamwise velocity and the wall velocity is observed at  $y^+ = 20$ .

A series of flow-visualisation pictures were obtained by Choi et al. (1998), which show the following details of the near-wall structure of the turbulent boundary layer when it is modified by the spanwise-wall oscillation. As the wall moves to the positive spanwise direction across the boundary layer during the oscillation, the Stokes layer containing a vortex sheet of positive streamwise vorticity is created near the wall surface. Without the freestream velocity of the boundary layer, the vortex-sheet contains only the streamwise vorticity component, pointing to the downstream direction. Combined with the freestream velocity of the boundary layer, however, the vortex-sheet vector is tilted to the positive spanwise direction with the movement of oscillating wall, generating a positive component of spanwise vorticity in the near-wall region of the boundary layer. As the wall moves to the opposite direction during the spanwise-wall oscillation, on the other hand, the Stokes layer containing a sheet of negative streamwise vorticity is produced. This time, the negative vortex-sheet vector is tilted in the negative spanwise direction during the wall oscillation, again creating a positive component of the spanwise vorticity. In other words, a positive spanwise vorticity  $\Omega_z$  is created in the near-wall region of the turbulent boundary layer during both positive and negative spanwise motions of the wall oscillation. There will be no net streamwise vorticity as a result of spanwise-wall oscillation, since the positive and negative vorticities during the wall oscillation are cancelled to each other. The numerical study carried out by Baron and Quadrio (1996) indeed shows the local maximum of the spanwise vorticity intensity at  $y^+ = 15$ , which seems to support the above argument that a positive spanwise vorticity is created in the near-wall region of the boundary layer as a result of the spanwise-wall oscillation (Choi et al., 1998).

A conceptual model for the boundary-layer profile with spanwise-wall oscillation is given in Fig. 9, demonstrating how the velocity profile can be affected by a spanwise vorticity in the near-wall region of the turbulent boundary layer. Here, the concentrated spanwise vorticity  $\Omega_z$  is located at  $y^+ = 15$ . At this

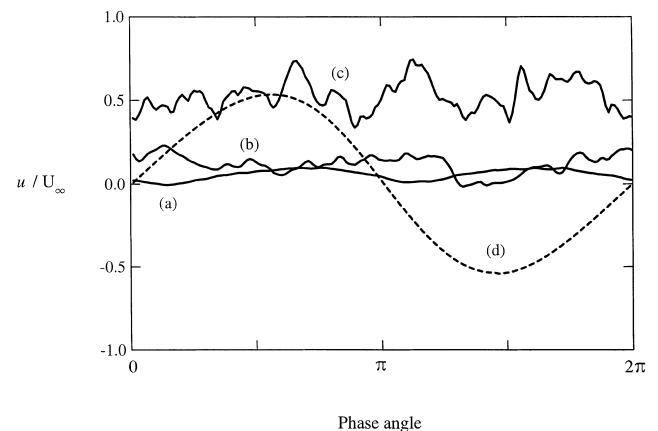


Fig. 8. Phase-averaged wall velocity (---) and streamwise velocity profiles with wall oscillation (over the oscillating plate,  $x = 350$  mm,  $\Delta z = 70$  mm,  $f = 6$  Hz): (a) at  $y^+ = 1.5$ , (b) at  $y^+ = 4$  and (c) at  $y^+ = 20$ .

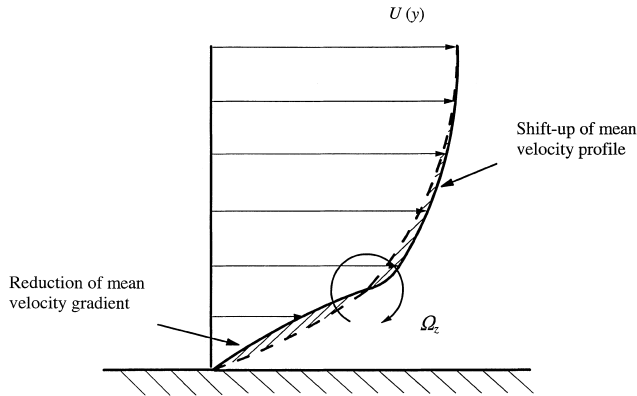


Fig. 9. Conceptual model for a turbulent boundary layer over an oscillating wall, showing a spanwise vorticity  $\Omega_z$  created by the periodic Stokes layer.

position of the boundary layer, the local spanwise velocity of the Stokes layer is totally out of phase with the wall velocity (Schlichting, 1968). This location also coincides with the peak of spanwise vorticity intensity of the boundary layer over an oscillating wall (Baron and Quadrio, 1996). As shown in this figure, the velocity profile near the wall ( $y^+ < 15$ ) is affected by the positive spanwise vorticity, in such a way that the mean velocity gradient is reduced by the induction velocity of the concentrated, positive spanwise vorticity. Outside the viscous sublayer ( $y^+ > 15$ ), on the other hand, the effect of the spanwise vorticity  $\Omega_z$  is to increase the mean velocity, shifting the logarithmic velocity profile of the boundary layer upwards (see Fig. 1). Both these changes in the mean velocity profile of the turbulent boundary layer were clearly observed in the experiments (Laadhari et al., 1994; Choi et al., 1998) as well as in the numerical simulations (Jung et al., 1992; Baron and Quadrio, 1996) with spanwise-wall oscillation.

Choi et al. (1998) also showed in their flow visualisation study that the longitudinal vortices in the near-wall region of the boundary layer move downstream in sinuous form as the test plate oscillates in the spanwise direction. This spanwise undulation of longitudinal vortices is caused by the Stokes layer over the oscillating wall, twisting the near-wall turbulence structure alternately with the change in wall direction during the spanwise oscillation. As a result, the streamwise vorticity associated with the longitudinal vortices in the near-wall region of the boundary layer is reduced. At the same time, the positive spanwise vorticity  $\Omega_z$  at the edge of the viscous sublayer created by the spanwise-wall oscillation (see Fig. 9) hampers the stretching of the longitudinal vortices in the viscous sublayer to reduce their streamwise vorticity. As a consequence, the *near-wall burst* (Choi, 1989) activity is weakened, leading to a reduction in turbulent skin-friction drag as observed in the present experiment. Indeed, it is found in the DNS results (Baron and Quadrio, 1996) that the intensity of streamwise vorticity fluctuations is nearly halved across the entire thickness of the boundary layer as the wall oscillates in the spanwise direction. It must be emphasised here that the changes in the mean velocity profile of the boundary layer by the spanwise vorticity  $\Omega_z$  do not lead to inflection points in the boundary layer profile (Choi et al., 1998). No increases in the level of the burst activity in the turbulent boundary layer are, therefore, expected as a result of wall oscillation.

Fig. 10(a) shows the conditionally sampled signature of the near-wall burst using the VITA technique (Blackwelder and Kaplan, 1976) at  $y^+ = 1.5$  over the oscillating wall. Here, the threshold of burst detection was set equal to the variance of the

velocity fluctuations ( $k = 1.0$ ) averaging over the non-dimensional integral time of  $t^+ = 10$ . The change in the burst signature is remarkable in the near-wall region of the boundary layer, where the duration of the burst is reduced to nearly one third of that without wall oscillation. A similar reduction in burst duration is observed at  $y^+ = 4$  (Fig. 10(b)). Even outside the viscous sublayer at  $y^+ = 20$  (Fig. 10(c)) the effect of wall oscillation on the burst signature is still significant, with the burst duration nearly a half of that without wall oscillation. Note that the vertical scale of the burst signatures (Figs. 10(a)–(c)) is normalised to allow a comparison of the behaviour of the velocity fluctuations to be made. It has been observed that the intensity of the near-wall bursts was greatly reduced by spanwise-wall oscillation.

#### 4. Conclusions

A wind tunnel study of the turbulent boundary layer with spanwise-wall oscillation was carried out, where reductions in skin-friction coefficient by as much as 45% were observed. With the logarithmic velocity profiles of the boundary layer shifted upwards and the turbulence intensities reduced by the spanwise-wall oscillation, the present results convincingly confirmed the basic conclusions of the recent direct numerical simulations. It was also shown that the skewness and kurtosis of the velocity fluctuations within the near-wall region are increased with a wall oscillation. The probability density functions of velocity fluctuations near the wall exhibited long tails of positive probability, reflecting the increases in the higher-moment statistics of the velocity fluctuations with the wall oscillation.

It was observed that the thickness of the Stokes layer was comparable to that of the viscous sublayer of the boundary layer when the turbulent drag reduction was observed with the wall oscillation. At the same time, the Reynolds number of the Stokes layer was found well below the critical value, so that the Stokes layer was expected to remain laminar if there were no boundary layers over the oscillating surface. These are considered to be important conditions in obtaining the turbulent drag reduction with spanwise-wall oscillation. This is because the modification of the near-wall structure seems to result from an interaction of the Stokes layer with the viscous sublayer of the turbulent boundary layer where the majority of the energy production takes place.

It is believed that the mechanism of drag reduction by spanwise-wall oscillation strongly relates to the spanwise vorticity generated at the edge of the viscous sublayer by the periodic Stokes layer. It was demonstrated in the present study that the positive spanwise vorticity created by the spanwise-wall oscillation reduces the mean velocity gradient of the boundary layer near wall. At the same time, the spanwise vorticity reduces the stretching of the longitudinal vortices in the viscous sublayer to reduce their streamwise vorticity. As a result, the near-wall burst activity, which is associated with the downwash of high-momentum fluid near the wall, is weakened leading to a reduction in turbulent skin-friction drag. A remarkable change in the burst signature in the near-wall region of the boundary layer was obtained using conditional sampling technique, where the duration of the burst is reduced to nearly one third of that without wall oscillation. The intensity of the near-wall bursts is also greatly reduced.

Although the present study was carried out in a wind tunnel, the basic findings from this research are equally applicable to liquid flows. Indeed, an experimental study has recently been carried out for turbulent pipe flow with water, where a section of the pipe was oscillated in the circumferential direction (Choi and Graham, 1998). The results indicated that

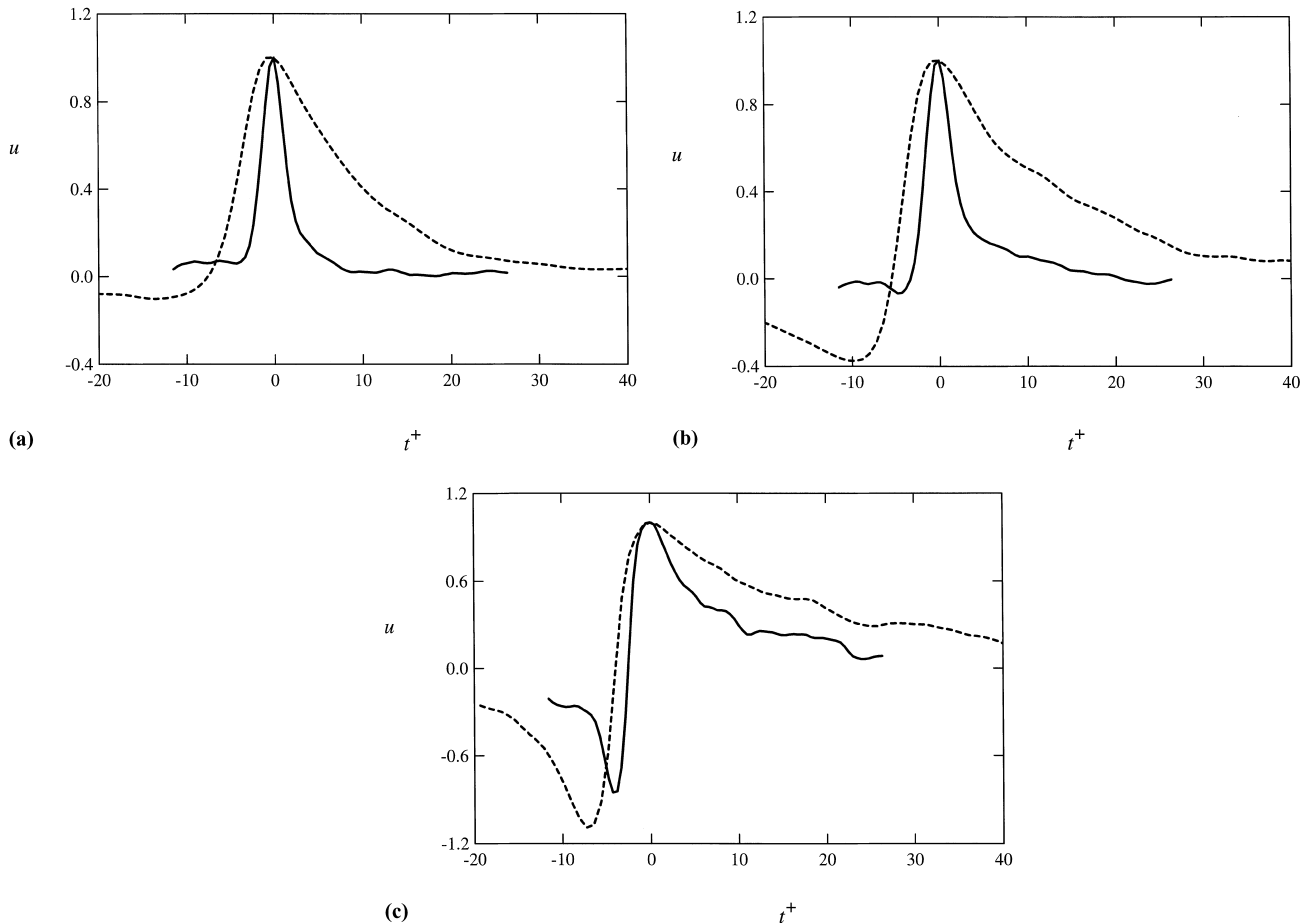


Fig. 10. (a) Conditionally sampled near-wall burst signatures (normalised) at  $y^+ = 1.5$ : – with wall oscillation (over the oscillating plate,  $x = 350$  mm,  $\Delta z = 70$  mm,  $f = 6$  Hz), --- without wall oscillation; (b) Conditionally sampled near-wall burst signatures (normalised) at  $y^+ = 4$ : – with wall oscillation (over the oscillating plate,  $x = 350$  mm,  $\Delta z = 70$  mm,  $f = 6$  Hz), --- without wall oscillation; (c) conditionally sampled near-wall burst signatures (normalised) at  $y^+ = 20$ : – with wall oscillation (over the oscillating plate,  $x = 350$  mm,  $\Delta z = 70$  mm,  $f = 6$  Hz), --- without wall oscillation.

the skin-friction factor of the pipe is reduced by as much as 25% as a result of active manipulation of near-wall turbulence structure by circular-wall oscillation. The turbulent pipe flows with circular oscillation have a great promise for industrial applications, such as in the transport of oil, gas, water and foodstuffs through pipes.

### Acknowledgements

Assistance of Dr. J.-R. DeBisschop and Dr. P.E. Roach during the course of research is appreciated. The work was supported by EPSRC Research Grants, GR/J06917 and GR/K27780 and some of the probes used in this investigation were made available from Rolls-Royce.

### References

- Akhavan, R., Kamm, R.D., Shapiro, A.H., 1991a. An investigation of transition to turbulence in bounded oscillatory stokes flows, Part 1. Experiments. *J. Fluid Mech.* 225, 395–422.
- Akhavan, R., Kamm, R.D., Shapiro, A.H., 1991b. An investigation of transition to turbulence in bounded oscillatory stokes flows, Part 1. Numerical simulations. *J. Fluid Mech.* 225, 423–444.
- Baron, A., Quadrio, M., 1996. Turbulent drag reduction by spanwise wall oscillations. *Appl. Sci. Res.* 55, 311–326.
- Blackwelder, R.F., Eckelmann, H., 1979. Streamwise vortices associated with the bursting phenomenon. *J. Fluid Mech.* 94, 577–594.
- Blackwelder, R.F., Kaplan, R.E., 1976. On the wall structure of the turbulent boundary layer. *J. Fluid Mech.* 76, 89–112.
- Choi, K.-S., 1989. Near-wall structure of turbulent boundary layer with riblets. *J. Fluid Mech.* 208, 417–458.
- Choi, K.-S. 1996. Turbulent drag reduction strategies. In: Choi, K.-S., Prasad, K.K., Truong, T.V. (Eds.), *Emerging Techniques in Drag Reduction*, MEP, London, pp. 77–98.
- Choi, K.-S., DeBisschop, J.-R., Clayton, B.R., 1998. Turbulent boundary-layer control by means of spanwise-wall oscillation. *AIAA J.* 36 (7), 1157–1163.
- Choi, K.-S., Graham, M., 1998. Drag reduction of turbulent pipe flows by circular-wall oscillation. *Phys. Fluids* 10 (1), 7–9.
- Dean, R.B., 1976. A single formula for the complete velocity profile in a turbulent boundary layer. *Trans. ASME J. Fluids Eng.* 98 (4), 723–727.
- Durst, F., et al., 1995. LDA measurements in the near-wall region of a turbulent pipe flow. *J. Fluid Mech.* 295, 305–335.

- Eaton, J.K., 1995. Effects of mean flow three dimensionality on turbulent boundary-layer structure. *AIAA J.* 33 (11), 2020–2025.
- Jeon, S., Choi, H., Yoo, J.Y., Moin, P., 1999. Space-time characteristics of the wall shear-stress fluctuations in a low-Reynolds-number channel flow. *Phys. Fluids* 11 (10), 3084–3094.
- Jung, W.J., Mangiavacchi, N., Akhavan, R., 1992. Suppression of turbulence in wall-bounded flows by high frequency spanwise oscillations. *Phys. Fluids A* 4 (8), 1605–1607.
- Kim, J., 1983. On the structure of wall-bounded turbulent flows. *Phys. Fluids* 26 (8), 2088–2097.
- Kline, S.J., Reynolds, W.C., Schraub, F.A., Runstadler, P.W., 1967. The structure of turbulent boundary layers. *J. Fluid Mech.* 30 (4), 741–773.
- Laadhari, F., Skandaji, L., Morel, R., 1994. Turbulence reduction in a boundary layer by a local spanwise oscillating surface. *Phys. Fluids A* 6 (10), 3218–3220.
- Pal, S., Deutsch, S., Merkle, C.L., 1989. A comparison of shear stress fluctuation statistics between microbubble modified and polymer modified turbulent boundary layers. *Phys. Fluids A* 1 (8), 1360–1362.
- Sarpkaya, T., 1993. Coherent structures in oscillatory boundary layers.
- Schlichting, H., 1968. *Boundary-Layer Theory*. McGraw-Hill, New York.
- Schoppa, W., Hussain, F., 1998. A large-scale control strategy for drag reduction in turbulent boundary layers. *Phys. Fluids* 10 (5), 1049–1051.
- Schwarz, W.R., Bradshaw, P., 1994. Turbulent structural changes for a three-dimensional turbulent boundary layer in a 30° bend. *J. Fluid Mech.* 272, 183–209.
- Sendstad, O., 1992. The near wall mechanisms of three-dimensional turbulent boundary layers. Ph.D. Thesis, Stanford University.
- Sherman, F.S., 1990. *Viscous Flow*. McGraw-Hill, New York.
- Smith, C.R., Schwartz, S.P., 1983. Observation of streamwise rotation in the near-wall region of a turbulent boundary layer. *Phys. Fluids* 26 (3), 641–652.
- Tennekes, H., Lumley, J.L., 1972. *A First Course in Turbulence*. MIT Press, Cambridge.